TALLINN UNIVERSITY OF TECHNOLOGY
SCHOOL OF ENGINEERING
Electrical Power Engineering and Mechatronics

STATOR INTER-TURN SHORT CIRCUIT FAULT DIAGNOSTICS OF ELECTRICAL MACHINES USING SPECTRUM ANALYSIS

ELEKTRIMASINATE STAATORI KEERDUDEVAHELISE LÜHISE RIKKEDIAGNOSTIKA SPEKTRIANALÜÜSI ABIL

MASTER THESIS

Student: Rinkeshkumar Prajapati
Student Code: 184512MAHM

Supervisor: Dr. Toomas Vaimann
(Senior researcher)
Co-supervisor: Mr. Bilal Asad
(Ph.D. student)

Tallinn 2020

AUTHOR'S DECLARATION

Hereby I declare that I have written this thesis independently.
No academic degree has been applied for based on this material. All works, major viewpoints and data of the other authors used in this thesis have been referenced.

"....."..... 20…..

Author: .....
/signature /

Thesis is in accordance with terms and requirements

"....."..... 20….

Supervisor: ….....
/signature/

Accepted for defence

"....."..... 20… .

Chairman of theses defence commission: .....
/name and signature/

Non-exclusive Licence for Publication and Reproduction of Graduation Thesis[1]

I, Rinkeshkumar Prajapati, 12/02/1996 hereby

1. grant Tallinn University of Technology (TalTech) a non-exclusive license for my thesis

Stator inter-turn short circuit fault diagnostics of electrical machines using spectrum analysis,

supervised by

Dr. Toomas Vaimann

Mr. Bilal Asad

1.1 Reproduced for the purposes of preservation and electronic publication, incl. to be entered in the digital collection of TalTech library until expiry of the term of copyright.

1.2 published via the web of TalTech, incl. to be entered in the digital collection of TalTech library until expiry of the term of copyright.

1.3 I am aware that the author also retains the rights specified in clause 1 of this license.

2. I confirm that granting the non-exclusive license does not infringe third persons' intellectual property rights, the rights arising from the Personal Data Protection Act or rights arising from other legislation.

---

[1] *Non-exclusive Licence for Publication and Reproduction of Graduation Thesis is not valid during the validity period of restriction on access, except the university's right to reproduce the thesis only for preservation purposes.*

_____ (*signature*)

_____ (*date*)

THESIS TASK

Student: Rinkeshkumar Prajapati, 184512MAHM

Study programme, MAHM02/18 - Mechatronics

main speciality:

Supervisor: Dr. Toomas Vaimann, Senior Researcher

Co-supervisor: Mr. Bilal Asad, Ph.D Student

Thesis topic:

(in English) Stator Inter-turn Short Circuit Fault Diagnostics of Electrical Machines using Spectrum Analysis

(in Estonian) Elektrimasinate staatori keerdudevahelise lühise rikkediagnostika spektrianalüüsi abil

Thesis main objectives:

1. To detect stator inter-turn short circuit fault at early stage
2. Spectrum analysis of three phase current space vector, speed, torque and also Park's vector approach

Thesis tasks and time schedule:

No	Task description	Deadline
1.	Understanding of the technical requirement	01/02/2020
2.	Motor design and simulation	25/03/2020
3.	Results analysis and writing	10/05/2020

Language: English **Deadline for submission of thesis:** 22/05/2020

Student: Rinkeshkumar Prajapati …… 2020

/signature/

Supervisor: Dr. Toomas Vaimann …… 2020

Co-supervisor: Mr. Bilal Asad …… 2020

/signature/

Head of study program: Prof. Mart Tamre …… 2020

/signature/

Abstract

In an induction motor (IM), commonly occurring faults are bearing, and insulation related faults, and rotor related and stator winding faults. Including this, stator inter-turn short circuit fault is the common key fault, which occurs due to ageing effect, contaminated lubricants, excessive loading, non-uniformity of the magnetic field, excess radial or axial forces, a partial short circuit in the windings, radial or axial misalignment between the motor and load, etc. That is why this work deals with the diagnosis of stator inter-turn short circuit fault of an IM. This kind of incipient faults needs to be identified and cleared as soon as possible to reduce failures as well as maintenance costs.

This thesis introduces a spectrum analysis for inter-turn fault detection in the stator winding of IM using Fast Fourier transform (FFT). The simulations are done in a finite element method (FEM) based environment (INFOLYTICA_MAGNET) to study the behaviours of the motor under healthy and faulty conditions. A MATLAB program is prepared for the comparison of various parameters taken from simulation for stator inter-turn fault cases. Three-phase current space-vector, torque and speed signals are used for the detection of short circuit faults. Two individual simulation data from a three-phase induction motor were recorded and analyzed by this method in MATLAB program.

Acknowledgement

From the profundity of my heart, I want to thank my spiritual mentors Rev. Pandurang Shastri Athvale (Dadaji) and Jayshree Talwalkar (Didiji) and God, without them I was unable to accomplish and finish this important task of my life. They are always a blessing for me for my potential knowledge and success. Their contribution to shaping my life is inexpressible as they have changed the lives of millions of people around the world.

I am thankful to my supervisor Dr. Toomas Vaimann and co-supervisor Mr. Bilal Asad, for their valuable guidance, support, sources and help during my thesis work. I also have best regards for TalTech faculties, including Prof. Mart Tamre, Mr. Dhanushka Liyanage, Mr. Even Sekhri and other teachers who had been helpful throughout my master's degree.

I would also like to express my gratitude towards my university and hostel friends for their contribution and experience and their ideas related to design, simulation and writing.

I am especially thankful to my family, friends, divine brothers, previous study teachers, FG OÜ job staff and relatives who have always provided me with the courage, strength, best wishes, moral and financial support during my study career.

Rinkeshkumar Prajapati
May 2020

CONTENTS

List of abbreviations and symbols

IM: Induction motor

FFT: Fast Fourier transform

FEM: Finite element method

MATLAB: Matrix Laboratory

DC: Direct current

AC: Alternating current

STIF: Stator inter-turn fault

SITSCF: Stator inter-turn short-circuit fault

PV: Park's Vector

FT: Fourier Transform

CM: Condition monitoring

FT: Fourier transform

PCA: Principal component analysis

DFT: Discrete Fourier transform

MCSA: Motor current signature analysis

SVM: Support vector machine

MEMS: Microelectromechanical system

MMF: Magneto motive force

EMF: Electromotive force

ANN: Artificial neural network

MLP: Multi-layer perceptron

GRNN: General regression neural network

MSE: Mean square error

SC: Short circuit

V/m: volt per meter

T: Tesla

C/m^2: Coulombs per meter squared

A/m: Ampere meter

A m-2: Ampere per square meter

H^{-1}: Inverse Henry

List of figures

List of table

1. Introduction

1.1 Overview

1.1.1 Electrical Machines

Induction motors, also named asynchronous motors, have an impact on almost every aspect of modern living. It is a sophisticated electro-mechanical device utilized in most industrial applications for the conversion of energy from electrical to mechanical form. Motors are used in almost every field dealing with electrical energy, such as industrial, mechanical, and manufacturing engineering fields. As compared to direct current (DC) motors, the use of IM both in industrial and domestic purposes is extensive, because they are robust, easily installed, controlled, and adaptable for many applications. The range size of the IM is from tiny to over 100,000 horsepower. Electric motors are the biggest consumer of electricity because their consumption is around 60% of global power. Overall electrical energy consumption by IM and the percentage of it in different sectors are shown in figure 1 [1].

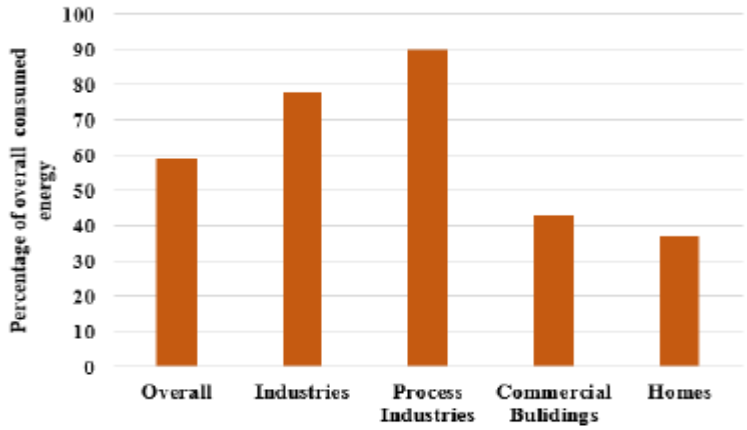

Figure 1 Energy consumption of IM in different sectors [1]

IM consists of three main parts, namely, rotor, stator, and enclosure. The main work is done by stator and rotor, and the enclosure protects the rotor and stator. The stator is the stationary part of an electric motor. It provides a rotating magnetic field that drives the rotating armature. For three-phase IM, the stator comprises of three-wire coils fixed inside a metal frame and spaced 120 electrical degrees apart. The stator windings are composed of connecting copper or aluminium conductor coil. The axis of the stator windings of a P-pole machine are spaced (2/P) (2π/3) mechanical radians apart, with each phase belt occupying the same number of slots. The terminals of the three-phase

stator winding can be a star (Y) or delta (Δ) connected [2]. The open model of the IM is shown in figure 2.

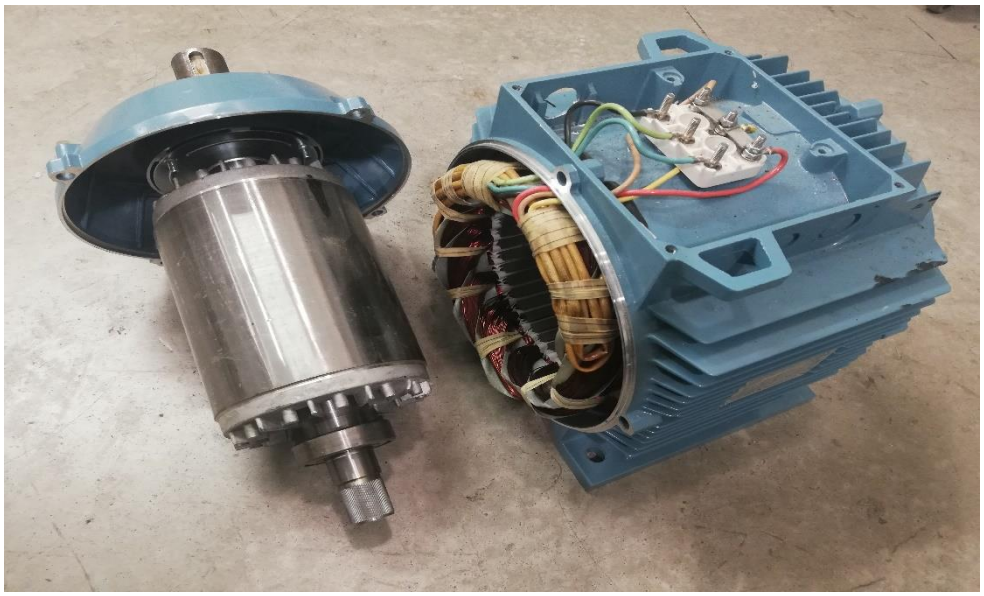

Figure 2 Stator (right) and Rotor (left) of IM

1.1.2 Main Faults

Electrical motors are associated with various parts that are always prone to failures. There are five types of failure modes in star connected stator [2].

A. Turn-to-turn short circuit fault
B. Coil-to-coil short circuit fault
C. Open circuit fault
D. Phase-to-phase short circuit fault
E. Phase-to-ground short circuit fault

Also, one of these modes or any combination of them can cause a fault. The turn-to-turn fault is the initial fault, and other faults can be regarded as the result of it. In the early stage, turn-to-turn fault does not affect the regular motor operation, because the voltage across the turn insulation is relatively low. However, high substantial transient voltage might cross the insulation, when the motor is switched ON or OFF. Thus, the destruction of turn insulation caused by the short circuit may cause permanent damage.

Different types of faults occur, which can cause unacceptable performance degradations and can be dangerous for personnel or equipment. Hence, early detection of fault is of significant importance. The fault detection in electrical machines and drive systems have

received remarkable attention. Initial detection of incipient faults prevents severe economic losses and ensures system reliability, stability, and safety. The damage of the motor can cause a big financial problem as well as energy waste. Sometimes this kind of significant fault can also cause an accident and can lead towards human injury. That is why, the monitoring of the motor is an essential task to prevent energy loss. Less energy waste will give more efficiency to the machine. The percentage contribution of different types of faults is shown in figure 3 [3].

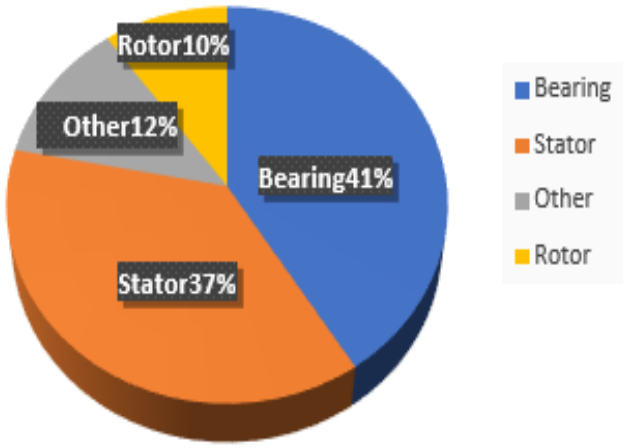

Figure 3 Percentage contribution of various faults in an IM [3]

1.2 Motivation

The reason for opting this specific topic was the broad approach to the tasks. As from the problem discussion, it is clear that this thesis requires enough research and analysis in the field of electrical machine design and faults analysis. The approach being used is going to be the new analysis technique to detect the stator inter-turn fault. This thesis is developing a fault detection technique, as discussed earlier. For this purpose, the author studied the different stator inter-turn fault (SITF) detection techniques to extract information and performed the analysis to select the best method.

1.3 Objective

As mentioned earlier, the stator is one of the significant fault areas in an IM, and it contributes to 37% of the total fault percentage of IM, as shown in figure 3. Early monitoring and diagnosis of these faults can have significant advantages like the safety of the operator, reducing production time loss, and minimizing the expensive maintenance and repair cost. To achieve this goal, the motor is modelled in the FEM environment (Infolytica_MagNet), and results are obtained of the three-phase current,

torque and speed for healthy as well as faulty cases and further processed them for space-vector, FFT and Park's Vector (PV) computation in MATLAB program. From the results of this analysis made a meaningful conclusion about the faults condition in IM.

1.4 Thesis Structure

This thesis is structured as follows; Chapter 2 reviews IM working and its basic parameters as well as relevant diagnostic techniques for SITF. This includes various fault diagnostic methods, as well as signal processing techniques. Chapter 3 introduces the design and simulation part of the IM, which comprises of a modelling technique called FEM. Chapter 4 presents the results obtained in two different cases that are healthy and faulty. Each case consists of the analysis of three-phase current, torque and speed. Finally, chapter 5 contains a discussion of the various results, their implication, conclusion, and suggestions for the future work.

2 Background

2.1 Induction Motor operation

The operating principle of an IM is based on the synchronously rotating magnetic field. The stator is composed of three windings electrically shifted 120ºe, as shown in figure 4. The three windings are connected to a three-phase ac power supply [4].

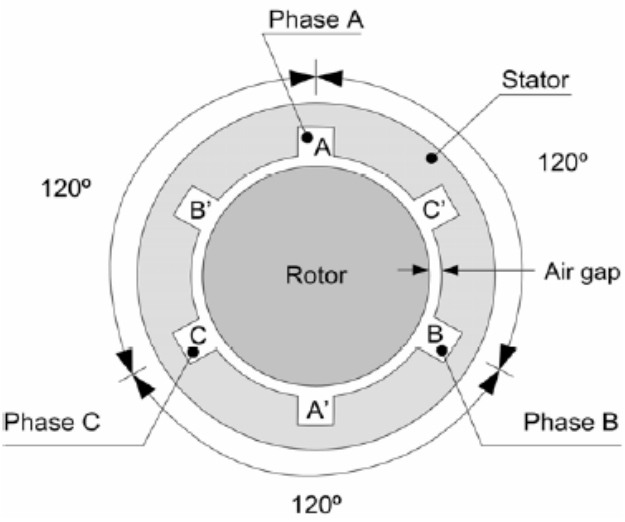

Figure 4 A two-pole IM schematic [5]

Powering the stator winding results in generation of magnetic flux in the stator which causes a flow of current in the coil. Rotor winding is designed such a way that, every coil becomes short circuited. The short circuited coil cuts the stator's flux in the rotor. Short circuit of the rotor coils follow Faraday's law of electromagnetic induction, and current starts flowing through the rotor's coil [6]. Flow of this current through the coil produces another flux in the rotor. Now, two fluxes are present, one is rotor flux and the other is stator flux. Stator flux will be leading with respect to the rotor flux. This will result in rotor having a torque that will make it rotate in the direction of the rotating magnetic field [6].

2.2 Parameters of Induction Motor

2.2.1 Voltage and Current

An IM is supplied by a three-phase AC system in which the three-phase currents are phase-shifted by 120ºe or 2π/3 electrical radians. The three-phase currents are thus defined as [4],

$$i_a = \overline{I}_m \cos\ (\omega t - \phi) \quad (2.1)$$

$$i_b = \overline{I}_m\ cos\ (\omega t - \phi - \frac{2\pi}{3}) \quad (2.2)$$

$$i_C = \overline{I}_m\ cos\ (\omega t - \phi + \frac{2\pi}{3}) \quad (2.3)$$

Where i_a - current in phase A in (Amp), i_b - current in phase B in (Amp), i_C - current in phase C in (Amp), $\overline{I}_m$ - peak fundamental frequency value of each phase current, ω - fundamental electrical angular frequency in (rad/s), ϕ - lag power factor angle in (electrical rad), and t – time in (sec).

The phase voltages are also phase-shifted by 120ºe or 2π/3 electrical rad. Considering the phase voltage, v_a, as a reference, the three-phase voltages are defined as [4],

$$v_a = V_m cos\ (\omega t) \quad (2.4)$$

$$v_b = V_m cos\ (\omega t - \frac{2\pi}{3}) \quad (2.5)$$

$$v_c = V_m cos\ (\omega t + \frac{2\pi}{3}) = V_m cos\ (\omega t - \frac{4\pi}{3}) \quad (2.6)$$

Where, v_a - phase voltage A in (V), v_b - phase voltage B in (V), v_c - phase voltage C in (V), and V_m - peak fundamental frequency value of the phase voltage.

The three-phase voltage system is defined in terms of the phase voltage (Vp) or the line voltage (v_L). The relation between VP and vl is defined as [4],

$$v_L = Vp\sqrt{3} \quad (2.7)$$

2.2.2 Synchronous Speed

For an IM with P poles, the synchronous speed is given in r/min as,

$$n_{syn} = \frac{120f}{p} \quad (2.8)$$

Where, f - stator frequency in (Hz), and n_{syn} - synchronous speed in (r/min).
However, the rotor rotates at an asynchronous speed, which is slightly slower than the synchronous speed. This difference between speeds is known as the slip speed, and it is given as [4],

$$n_s = n_{sys} - n_{asyn} \tag{2.9}$$

Where, n_{asyn} - asynchronous speed in (r/min), and n_s - slip speed in (r/min).

2.2.3 Flux Linkage

Flux linkage is used in the electromagnetic analysis to represent the number of magnetic lines crossing an electrical circuit, such as a coil. The magnetic flux linkage ψ is given as [4],

$$\psi = \int N d\emptyset \tag{2.10}$$

Where N - number of turns of a coil, and ψ - magnetic flux in (Wb). Thus, the flux linkage is given in Wb-turns. From Faraday's Law, an electromagnetic force (emf), e, is induced in an electrical circuit due to changes with time in the amount of flux linkage linking that circuit such that,

$$e = -\frac{d\psi}{dt} \tag{2.11}$$

2.2.4 Torque

Torque is the force needed to turn a shaft times its arms-length to the axis of rotation. Thus, torque (T) is given by [4],

$$\mathrm{T} = \mathrm{F_R} \tag{2.12}$$

Where F - force in Newton (N) applied to a shaft, and r is the arm length of the force. The torque in an IM is produced from the interaction of the resultant air-gap flux and the MMF (magneto motive force) of either the stator winding or the rotor cage. Torque is produced on the shaft of the motor only if the rotor is running at speed lower than the synchronous speed, i.e., if the slip speed is a nonzero value.

2.3 Space-Vector

A common three-phase electrical system comprises of a set of three voltages and currents interacting with each other to deliver electrical power. A practical three-phase system cannot be considered as the simple addition of three independent single-phase subsystems. Particular relations exist between the phase variables of a three-phase system, such as those resulting from the Kirchhoff laws or regarding phase sequences, which invite the application of certain space vector transformations to obtain a more elegant and meaningful representation of its variables.

The space-vector analysis is based on the transformation of a set of three-phase variables into a space vector (complex variable). In steady-state conditions, such transformation is related to the traditional symmetrical component. When space-vector theory is applied, the various transformation models can be obtained without performing matrix transformation [7]. The space-vectors for the balanced three-phase sinusoidal signal is described as [8],

$$f_A = cos(\omega t),\ f_B = \cos(\omega t - \alpha),\ f_C = \cos\ (\omega t + \alpha) \tag{2.13}$$

Where $\alpha = \frac{2\pi}{3}$

The corresponding space-vector is,

$$f_R = (f_A + \gamma f_B + \gamma^2 f_C) = 1.5e^{j\omega t} \tag{2.14}$$

Where $\gamma = e^{j\alpha}$

2.4 Literature Survey

Many surveys have been proposed, and significant endeavours have been dedicated to IM fault diagnosis during the last one to two decades [9-19]. Thus, a short description of the main methods discussed in the literature is summarized in this section.

2.4.1 Off-line Monitoring

Off-line methods are typically more direct and accurate. For IM motors, user does not require in-depth knowledge of electrical machines. Testing can be done through a basic understanding of electrical tools. An advantage of off-line monitoring is that it can carry out meaningful tests after the manufacturing of the unit. This method works only with the static condition of the motor and does not allow observing the state of IM in dynamic condition [9].

2.4.2 On-line Monitoring

For a continuous process application, such as petrochemical, water treatment, management of materials, etc. on-line control diagnostic techniques are preferred. The benefit of this procedure is that a machine will not require to be taken out of service. As a result, a person can measure the reasonable operating condition, while the machine is running. On the other hand, it requires the installation of additional equipment to operate [9].

2.4.3 Using Fast Fourier Transform

In this research [10], the author discussed Fourier transform (FT), which is the operation of decomposing a function (or signal) from time into its frequency components. To find the fault in frequency component, the author provides the methodology using principal component analysis (PCA) to cater to the feature of the FFT signal and utilize the Hotelling's T2 as an index for fault detection. After selecting the top five peak frequencies and corresponding amplitude of the FFT as a feature and reducing the dimension through PCA, it is possible to detect a motor abnormality through Hotelling's T2 value.

A PCA reduces dimensions while maintaining necessary information about huge data cause of its multivariate statistical analysis feature. As a result, it improves fault detection and diagnostic ability to detect the fault signal. This research paper prefers the algorithm that uses the PCA to find the probability bounds of the variations of the peak frequencies and relative values of the FFT by Hotelling's T2 value [10].

2.4.4 Wavelet Techniques

In the research paper, "Stator fault diagnosis and protection in three-phase IM based on wavelet theory" [11], Adel and Khalid proposed an approach for diagnosing stator fault types from three-phase stator currents based on wavelet packet transform. The signal processing method of the FFT technique depends on the stator current fundamental frequency, motor speed, and load. These are enough to analyze, but sometimes they cannot be applied for high sharp signals with nonlinear systems. While the wavelet technique is capable of getting information in frequency and time domains, it is also highly sensitive for diagnosis faults as compared to classical signal processing methods like a Discrete Fourier transform (DFT) and FFT. These methods are based on applying digital signal processing tools on stator currents of IM [11].

The above-cited method works on the principle that all signals can be reconstructed from the sets of local signals of varying scale and amplitude, but its shape remains constant [11]. In contrast to sinusoids, wavelets are localized in the time and frequency domains, so wavelet signal processing is suitable for these signals, there the spectral content changes over time. Wavelet signal processing is different from other signal processing methods because of the unique properties of wavelets. e.g., wavelets are not regular in shape and finite in length [12]. The benefit of using wavelet techniques for fault monitoring and diagnosis of IM is enhancing because such procedures allow us to perform stator current signal analysis during transients [12].

2.4.5 Motor Current Signature Analysis (MCSA)

Authors, namely Luqman, Zakariya, and Mohammed, discussed the MCSA technique [13]. This technique is considered one of the great fault diagnostic techniques for detecting the faults in electrical machines. This technique is suggested for safe performance and to improve the efficiency of IM. This method works for obtaining current and voltage signals of the stator, which are considered for signature analysis of IM. The stator current signals measured from the motor are proceeded further to the power spectrum profile to determine the cause of IM failure. These kinds of current and voltage signals are measured by current and voltage sensors, and then the advanced tools such as artificial neural networks, digital signal processing devices, fuzzy logic, etc. are applied [13].

To detect the stator inter-turn fault, the fault signatures of currents and voltages space-vectors are compared at corresponding spectrums. To get the fault harmonics from both current and voltage space-vectors, complex FFT is applied. The load torque, speed variations, and the fault severity effects on the fault signatures can be used to detect the inter-turn short circuit fault and determine their fault severity.

2.4.6 Current Coordinate Transformation

In another research paper [14], the author considered a dynamic method of the stator winding inter-turn short circuit identification, which is not based on current spectral analysis. This research defines the technique of identifying the short circuit failure in the stator of the asynchronous three-phase motor, which relies on the coordinate transformation of the current vector.

The maximum integrated current can be analyzed by the angle of the ellipse axis in the indication unit algorithm. With this result, one can conclude the state of winding. In the diagnosed IM, one winding was shorted 1:30 part of the previous winding. The angel of rotation signal becomes nearby zero after fine-tuning. PI regulator in feedback the maximum integral of stator current in fault phase varies from the mean value by 2.4%, and it shows an inter-turn short circuit in the period. Stator current of the fine motor without inter-turn circuit produces flow between phases, which is not greater than 0.2%. The advantage of this proposed method is its simplicity with less data array processing in the algorithm of the developed diagnostic system [14].

2.4.7 Using Distortion Ratio

Shrinathan, Yukio, and Hisahide presented [15] analysis of characterizing the amplitude of the load current and considering it to be the main feature for diagnostics. However, using this method, it is only possible to detect two or more failures. Generally, in the case of low voltage IM, if a minor short circuit fault occurs, such as one turn short circuit insulation failure, the motor will not immediately result in a fatal electrical breakdown and continue to operate for a certain period even with the presence of a fault. For this kind of fault, the authors provide a diagnostic method in this paper [15].

The diagnostic system proposed for detecting one-turn short circuit insulation failures using a support vector machine (SVM). The proposed method has difficulty in diagnosing faulty motors under the no-load condition because the amplitude of the frequency spectra between the two motors shows no remarkable difference [15].

2.4.8 Vibration Signals by MEMS Accelerometer

In this research paper [16], it shows the technique for identifying inter-turn fault in three-phase IM stator winding by vibration analysis using microelectromechanical systems (MEMS) accelerometer. The short circuit of the stator winding leads to an effect on the main air-gap flux distribution. The fault current due to the shorted turn is the source of an additional MMF pulse, which also has harmonic space distribution superimposed on the main field distribution.

An increase in the magnitudes of fault frequency indicates the severity of the fault. From this paper, it has been proved that MEMS accelerometers can be successfully employed to detect the stator winding short circuit fault in IM. This method is simple and non-electrical contact type method which is free from electrical hazards [16].

2.4.9 Torque Analysis

In this work [17], it indicates the diagnostic result of torque pulsation under the inter-turn short circuit of three-phase IM during the initial stage. In the research, three techniques were used: finite element analysis, signal analysis, and artificial neural networks (ANN). This paper describes the effect of inert-turn short circuits on torque pulsation in transient state. Torque waveforms for both healthy and faulty motor were calculated. The calculations were carried out in Maxwell computing software. By using the wavelet technique, obtained waveform have been analyzed. Torque waveforms of torque pulsation, under inter-turn short circuit, were made.

In the case of a loaded motor by rated torque, the fault of multi-layer perceptron (MLP) is lower than that of an unloaded motor. Regardless of the motor load, MLP generates more substantial errors than the general regression neural network (GRNN). Moreover, the GRNN influence of spread on mean square error (MSE) is significant only for a small number of shorted turns. Increasing the number of shorted turns reduces the effect of the spread parameter on the MSE [17].

2.4.10 Artificial Intelligence (AI)

Artificial intelligence (AI) methods have been presented according to many surveys, using ideas such as fuzzy logic [18] and genetic algorithms [19]. The AI-based technique not only classifies the faults but also identify the fault severity. These methods build offline signatures for each motor operating condition and an online signature for the status of a motor being monitored. A classifier compares the formerly stored signatures with the signature generated online to classify the motor operating condition and identify the fault severity. However, most of such AI-based techniques require large datasets. These datasets are used to learn a signature for each motor operating condition that is considered for classification. Thus, a large amount of data is required to train such algorithms to cover the most common motor operating conditions and obtain good motor fault classification accuracy. Moreover, AI-based techniques for motor fault classification may not be adequately robust to classify faults from different motors from those used in the training process. Additionally, such datasets are usually not available, involve destructive testing, and considerable time to generate.

The new method for SITF is the subject of this thesis "Stator inter-turn fault diagnosis of IM using spectrum analysis". For this research work initially, the current, torque, and speed results were recorded. These results were processed in MATLAB program to get space-vector and FFT. The faulty condition of the motor known by comparing the harmonics in the frequency spectrum of the different signals results.

3 Simulation

3.1 FEM Based Simulation

The mathematical modelling and simulations of IM are essential, as it is a fundamental milestone for design and control procedures. The more accurate the mathematical model of the machine is, the more precise its practical design and control would be. With the increase in computational power, numerical models such as FEM, are gaining more and more popularity in the field of modelling and simulations. These models are good approximations of an actual system, as they consider all possible parameters, but at the cost of complexity and long computational time. The numerical model of the IM depends on Maxwell's equations [20],

$$\nabla \times \mathrm{E} = -\frac{\partial \mathrm{B}}{\partial \mathrm{t}} \tag{3.1}$$

$$\nabla \times \mathrm{H} = \mathrm{J} + \frac{\partial \mathrm{D}}{\partial \mathrm{t}} \tag{3.2}$$

$$\mathrm{H} = \nu \mathrm{B} \tag{3.3}$$

$$J = \sigma E \tag{3.4}$$

Where E - electric field strength in (V/m), B - magnetic flux density in (T), D - electric flux density in (C/m^2), H - magnetic field strength in (A/m), J - current density (Am-2), v - magnetic reluctivity of material in (H^{-1}) and σ - electric conductivity.

By assuming that the magnetic field lies in an x-y plane and varies sinusoidal in time and induces currents in the z-direction, the vector potential A distributes in the machine according to the following equation [20],

$$\frac{\partial}{\partial \mathrm{x}}\left(\frac{1}{\mu}\right)\frac{\partial \mathrm{A}}{\partial \mathrm{x}} + \frac{\partial}{\partial \mathrm{Y}}\left(\frac{1}{\mu}\right)\frac{\partial \mathrm{A}}{\partial \mathrm{Y}} - \mathrm{S}\frac{\partial}{\partial \mathrm{x}}(\sigma \mathrm{A}) + \mathrm{J} = 0 \tag{3.5}$$

If the conductivity of the rotor and stator laminations is taken as zero, and the reluctivity of conducting regions like that of the vacuum, the electric scalar potential and voltage equation of a conductor can be represented as [20],

$$\nabla \varphi = -\frac{u}{t} e_z \tag{3.6}$$

$$\mathrm{u} = \mathrm{iR} + \oint \sigma \frac{\partial \mathrm{A_z}}{\partial \mathrm{t}} . \mathrm{ds} \tag{3.7}$$

Where σ - conductivity of conducting material, A - vector potential, R – resistance in (ohm), *i* - current and u - voltage.

The FEM is the most commonly used method for solving problems of engineering and mathematical models. This FEM is a particular numerical method, that is used to solve partial differential equations in two or three space variables. The FEM subdivides an extensive system into smaller, more unaffected parts that are called finite elements. This is achieved by a particular space discretization in the space dimensions, which can be implemented through the construction of a mesh of the object in the numerical domain for the solution that has defined several points. This finite element method formulation of a boundary value results finally in an algebraic equation. The method assumes the unknown function over the domain. This simple equation that model these finite elements are then assembled into a more extensive system of equations that designs the entire problem. The subdivision of a whole domain into more unaffected parts has several advantages such as [21],

- Accurate representation of complex geometry
- Inclusion of dissimilar material properties
- Easy representation of the total solution
- The capture of local effects

3.2 Design and Simulation

3.2.1 Structure of IM

The work has been carried out with Finite element based simulation. The studied model takes its geometrical and materials characteristics from a 400 V, 7.5 kW, 50 Hz, 3-phase IM. The stator slot number is 36, and the rotor slot number is 28. Due to the long simulations to acquire steady-state signals appropriate for signal processing, the simulated models have been analyzed in 2D.

In order to create an IM according to the datasheet, used INFOLYTICA (MagNet) software. A MagNet is a powerful tool where one can design a motor and perform 2D and 3D models for magnetostatic, time-harmonic, transient, or transient with motion analysis with a reasonably good degree of accuracy. Magnet uses the finite element technique to measure an accurate and quick solution to Maxwell's equations. Each module is tailored to simulate different types of electromagnetic fields [22].

The required geometry is drawn using the corresponding tools. For example, using the circle tool to draw the circle of different radius and with the help of line and arc tools, draw the pattern of slots. The IM with 36 stator slots, 28 rotor slots, and four poles, which is to be designed, and its design parameters are listed out in Appendix 1. All dimensions shown are in millimeters (mm). The parameters are fixed to the component, and the necessary materials are filled in the component like soft pure iron for shaft, rotor steel for stator and rotor, aluminium for rotor bar and copper for stator slot.

To design a machine, it is necessary to know the physical meaning of all the dimensions of the machine. Dimensions of the motor are as follows [23].

Stator outer diameter: The maximum distance between the center of the motor and the stator outer circumference is called the stator outer radius. Twice, the stator outer radius is the stator outer diameter.

Stator inner diameter: The maximum distance between the center of the motor and the stator inner circumference is called the stator inner radius. Twice, the stator inner radius is the stator inner diameter.

Rotor outer diameter: The maximum distance between the center of the motor and the rotor outer circumference is called the rotor outer radius. Twice, the outer rotor radius is the outer rotor diameter.

Rotor inner diameter: The maximum distance between the center of the motor and the rotor inner circumference is called the rotor inner radius. Twice, the rotor inner radius is the rotor inner diameter.

Air gap: Air Gap is the gap between the rotor outer circumference and the stator inner circumference.

3.2.2 Stator Slot and Coil

The active part is modelled, as shown in figure 7. The motor is not only dependent on active geometry but also somewhere connected between the remaining electrical parameters. This is done in INFOLYTICA software by building up slots and required circuit. Appendix 1 shows the stator slots dimension. 36 slots were created by following those dimensions.

Coils are then created by using the Model tool and "Make a simple coil" option. The parameters of the coil are then set. The stator is made of steel laminations, and they are stacked together. Figure 5 shows the stator winding configuration. The stator coil

circuit diagram is shown in appendix 2. The winding configuration details are shown in table 1.

Table 1 Stator winding configuration

Each phase has six coils in series due to numbers of poles	4
The number of slots per pole and phase	4
The total number of stator slots	36
The total number of slots per phase	12
Full pitch	36/4 = 9
Coil pitch	7/8/8/8/8/7/

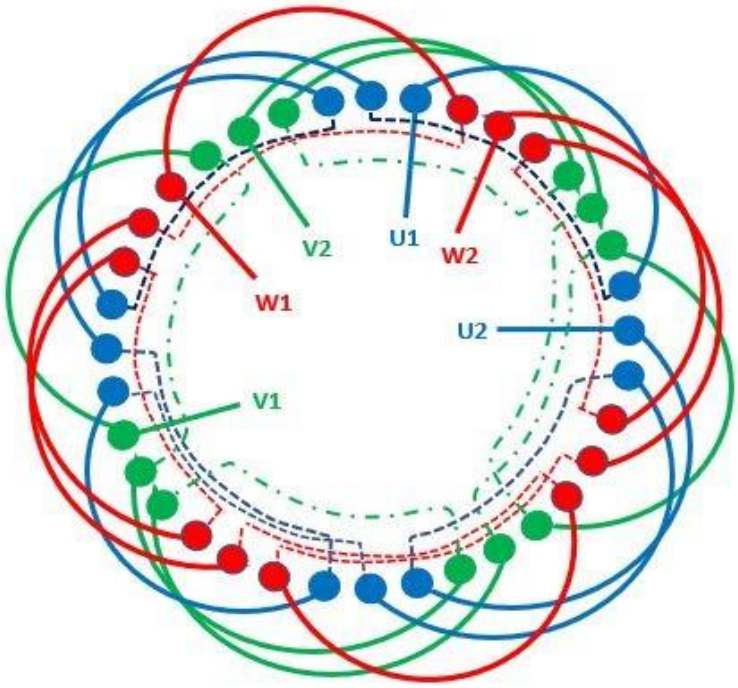

Figure 5 The stator winding configuration

3.2.3 Rotor Slot and Coil

The same thing has been done with the rotor slot. Appendix 1 shows the rotor slot dimension. Figure 6 shows the circuit diagram for rotor coils, where the additional resistances are needed to complete the circuit. This is because the simulation is 2D, and the short-circuiting end rings are neglected. The value of the resistance calculated based on rotor slot area and the final value has set in the circuit. The value of resistance will be the same for 28 rotor coils. The rotor bar coils are selected as a solid type.

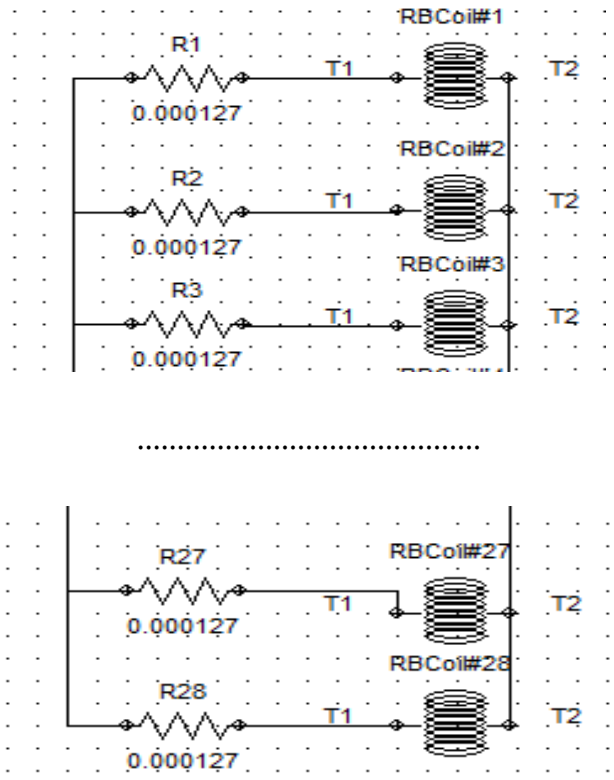

Figure 6 Rotor coils with resistance

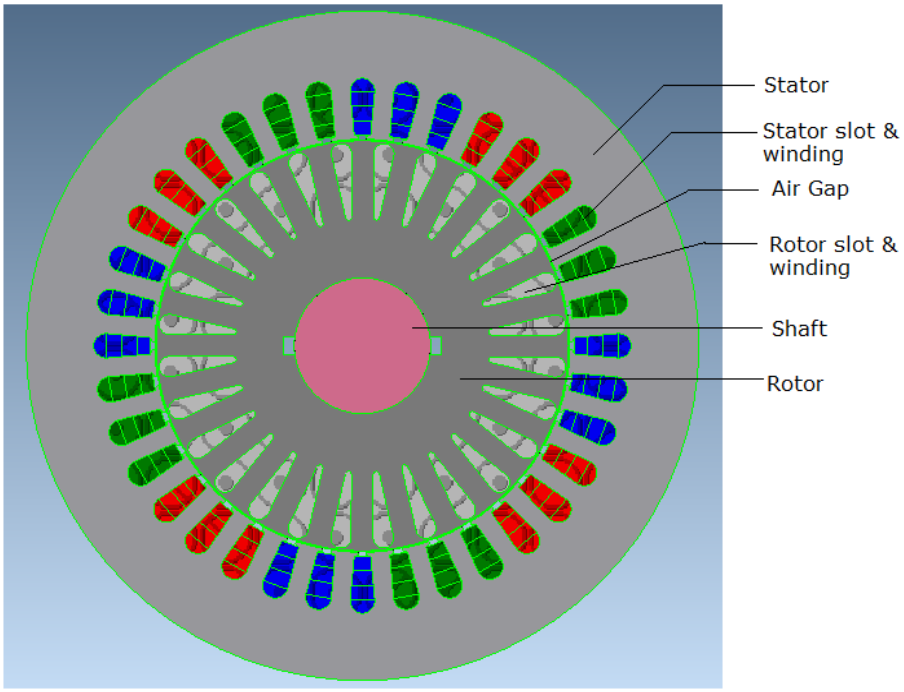

Figure 7 Completed IM Model

After completing the different steps such as, wireframe model, assigning different materials for different parts, stator and rotor coils connection, the final healthy IM model is shown in figure 7.

3.2.4 Mesh Analysis

FEM mesh created by the analyst before finding a solution to a magnetic problem using FEM, which is shown in figure 8. The meshes will introduce these elements to the model. Every region is subdivided into finite elements, and Maxwell's equations will be solved for these entire regions. Different colors indicate that the analyst has set material properties for each zone. This geometry may seem simple; it would be very challenging to calculate the magnetic field for this setup without FEM, using equations alone. The total numbers of elements are directly proportional to the solving time, and FEM simulation is already well known for its lengthy computation time.

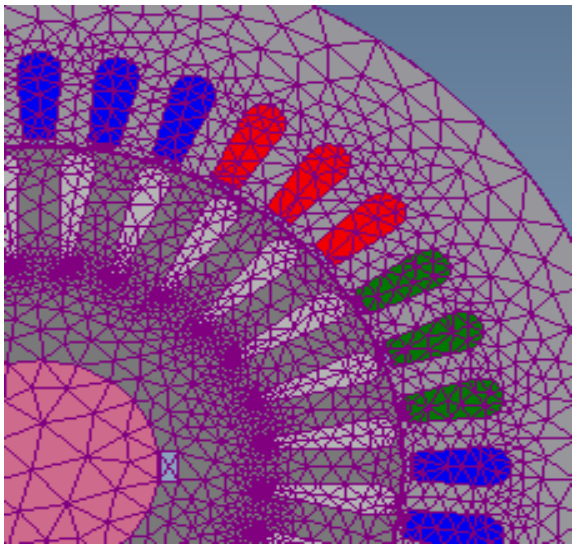

Figure 8 Mesh Solution Model

3.2.5 Stator Winding Short Circuit Model

The stator winding inter-turn short circuit fault consists of two types, one is the inter-turn short circuit in the same coil, and the other is an inter-turn short circuit in the different coil. For the inter-turn short circuit fault in the same coil, taking stator slot CoilA13_4. The slot A13 consists of four coils, namely CoilA13_1, CoilA13_2, CoilA13_3, and CoilA13_4. For inter-turn short circuit fault in the different coil, taking stator slot CoilA'13, e.g., slot A'13 consists of four coils, namely CoilA'13_1, CoilA'13_2, CoilA'13_3, and CoilA'13_4. The short circuit model is shown in figure 9, in which shorted coils are marked by a black arrow. An external circuit with one coil short circuit should be introduced, which is shown in figure 10. For the inter-turn short circuit in different cases, both coils should be divided, and the settings should be made in the external circuit diagram. The final results of current, speed, and torque in healthy, as well as faulty cases, are discussed in the next chapter.

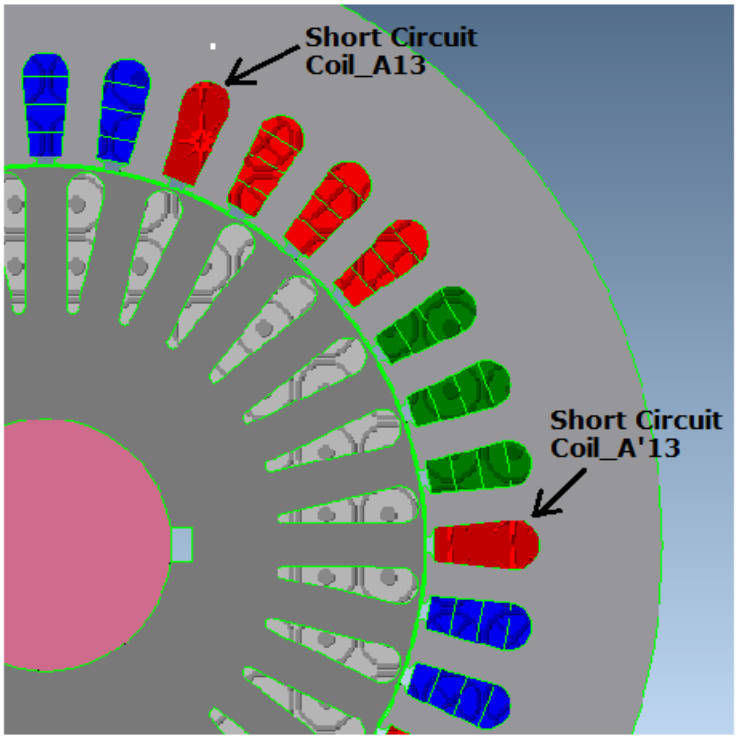

Figure 9 Short circuit model of IM

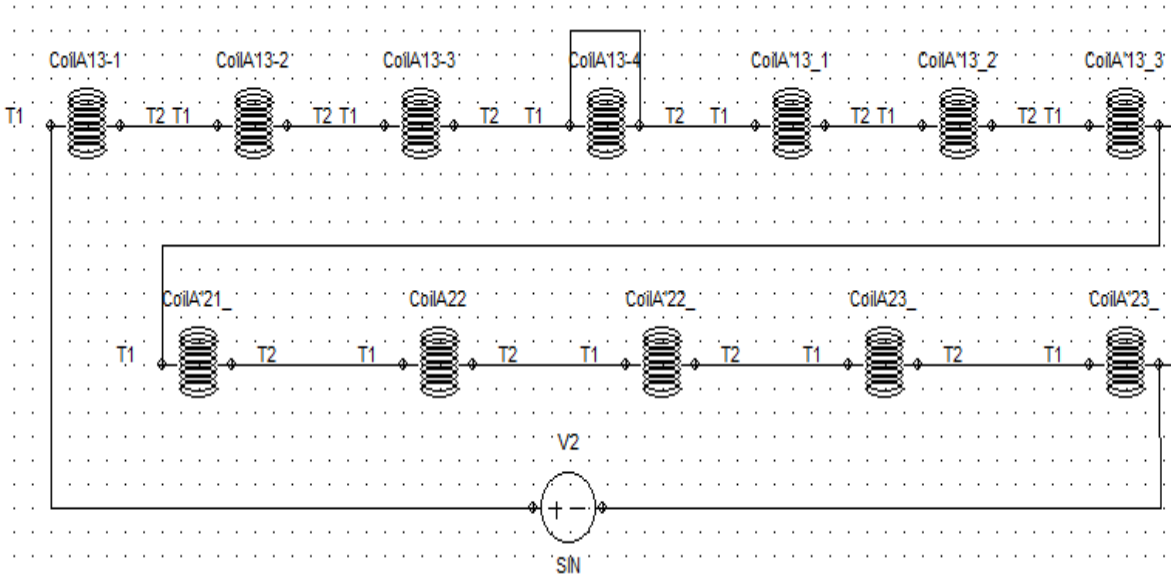

Figure 10 Stator coil connection in short circuit case (Phase V2)

The simulation is done based on the genuine IM design, which means that it is an approximate replica because of the following assumptions. All the dimensions and features of the machine are considered to an extent which is known to the author. There are various important remarks which are indispensable to highlight prior to the actual simulation results [20],

- It is a two-dimensional (2D) machine. The end rings are excluded, and the interconnection of the rotor bars is done through the electrical circuit, as shown in figure 6. To compensate for the end winding regions, the series-connected resistances and inductances are used.
- The effective length of the machine is 155 millimeters.
- The current source considered as an ideal for the circuits.
- Stator and Rotor coils connections are in star.
- Used constant load throughout the simulations is 49 Nm.
- Simulations are done with 2200 ms and the sampling frequency of 20 kHz.
- Stator winding used in the simulation is shown in Appendix 2.
- The motor is no longer symmetrical because of the fault in it. The simulation needs to be done for entire geometry rather than taking one symmetrical sector, which increases the simulation time considerably.

4 Results

To verify the considered diagnostic methods, several healthy and fault conditions in the simulation were introduced. In this simulation, three types of analysis were used. Firstly, the healthy motor, secondly one coil short circuit, and lastly three coil short circuit. The simulation consists of a 7.5kW, 690/400V, induction motor with the stator windings in star connection. The stator windings were changed to get several accessible tapings that can be used to create inter-turn short circuits, with different turns and different locations along the stator windings. Simulation tests were performed using the MATLAB program for space-vector as well as for FFT method with 5 kHz sampling frequency to get the spectrum. The use of spectrum analysis is to transform the measured time-domain signal into a frequency-domain signal to analyze. The simulation results of the IM under the healthy and faulty conditions are discussed below.

4.1 Signal Processing

In terms of signal processing, one important factor to consider is that the sampling process must meet the conditions of the sampling theorem so that the resulting sequence contains all the information of the original signal [24]. Another signal processing phenomenon relevant for the analysis is the computation of amplitude versus frequency spectrum of different signals using FFT function in MATLAB program.

4.2 Electrical Characteristics of Inter-Turn Fault

An electrical circuit diagram in figure 10 shows a three-phase stator winding under short circuit condition assumed in phase 1. The two circuits are electrically independent and magnetically coupled. When the short circuit occurs, the shorted turns physically act as a shorted coil placed in the machine's main magnetic field path. An electromotive force (EMF) is thus induced in these driving a fault current. Due to Lenz’s law, the fault current establishes a flux opposing that of the main field, consequently reducing it along with the faulty coils, and in turn, reducing EMF. Another effect which reduces EMF is the main MMF reduction due to fault-induced reduction of ampere/turns in the faulty phase [25].

4.3 Analysis of Simulation Results

4.3.1 Flux Distribution

Figure 11 shows the flux distribution of the IM under healthy conditions. All the four poles of the IM are visible, and magnetic distribution between the poles is in good correlation. There are no significant variations between the poles. The motor is shown

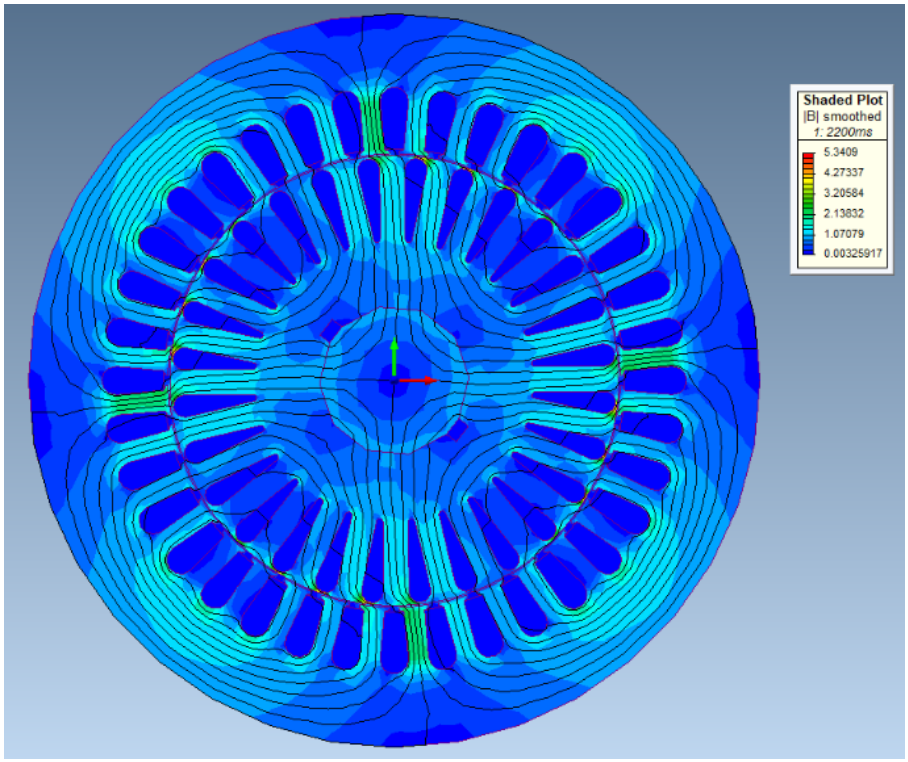

Figure 11 Magnetic field density of health motors

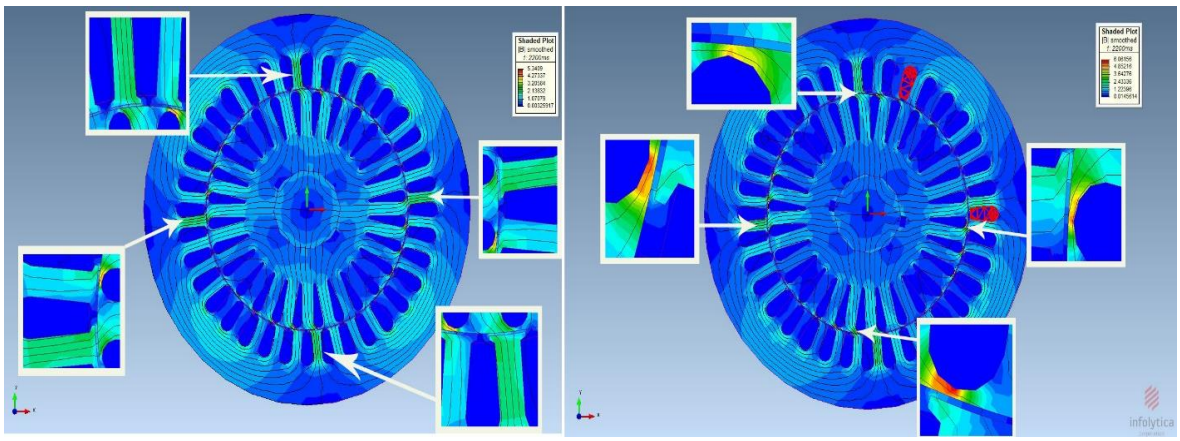

Figure 12 Magnetic field density of healthy and stator inter-turn short-circuit motor

the right side of figure 12, has a short circuit fault which is marked by red color. When looking at the magnetic distribution on the inner side of the motor, it seems all good. But when taking a closer look at stator bar numbers 3 and 10, and their neighboring bars 2 and 11 and comparing them, there is a little variation detectable in magnetic field distribution. This non-uniform flux distribution increases stray flux, which passes through bearing and produces eddy current in them. If these eddy currents prolong for a long time, then they can damage the inner and outer races of bearing.

4.3.2 Three-Phase Current

The first simulation with the motor in a healthy condition was performed. To perform the analysis during a healthy state, a three-phase supply current was taken, which is in the form of the time-domain. Then space-vector analysis was performed. Afterwards, processed these currents through FFT to get the results in the frequency-domain. For FFT, the sampling frequency of 5kHz was selected. When the motor runs with no faults, the behavior of the IM is perfectly normal, and the spectrum of the motor supply currents does not contain any harmonics. Figure 13 shows the three-phase current in time-domain during a healthy state. Figure 14 and 15 shows the simulation results in the frequency-domain when the motor runs in healthy conditions.

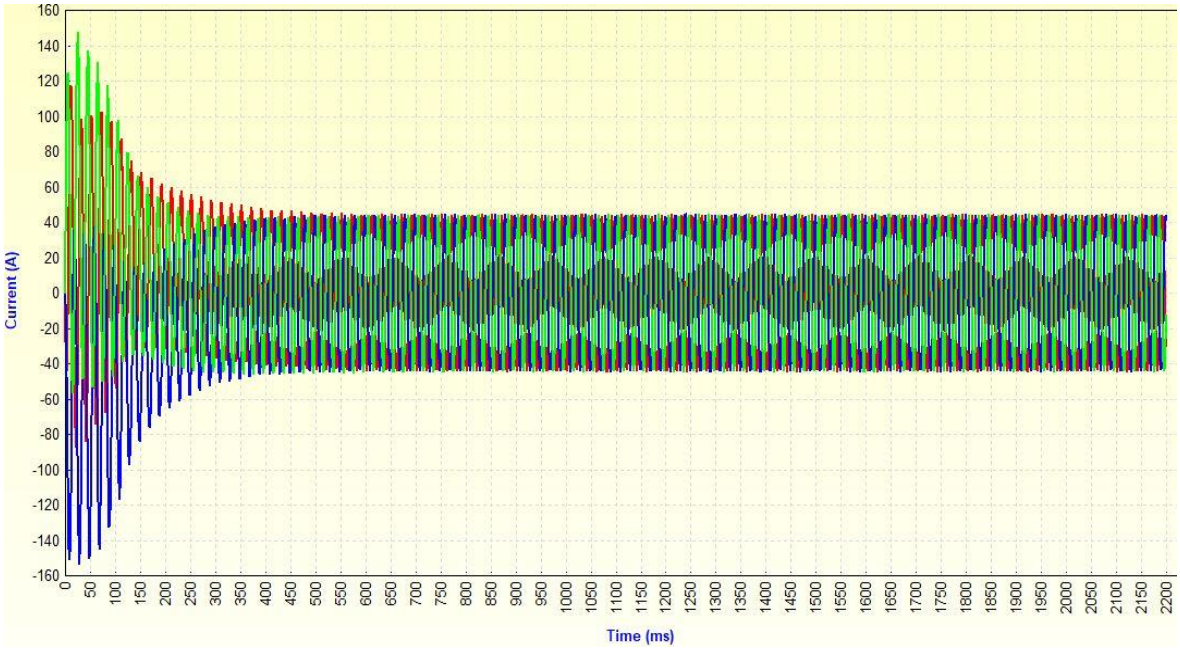

Figure 13 Three-phase current under healthy case

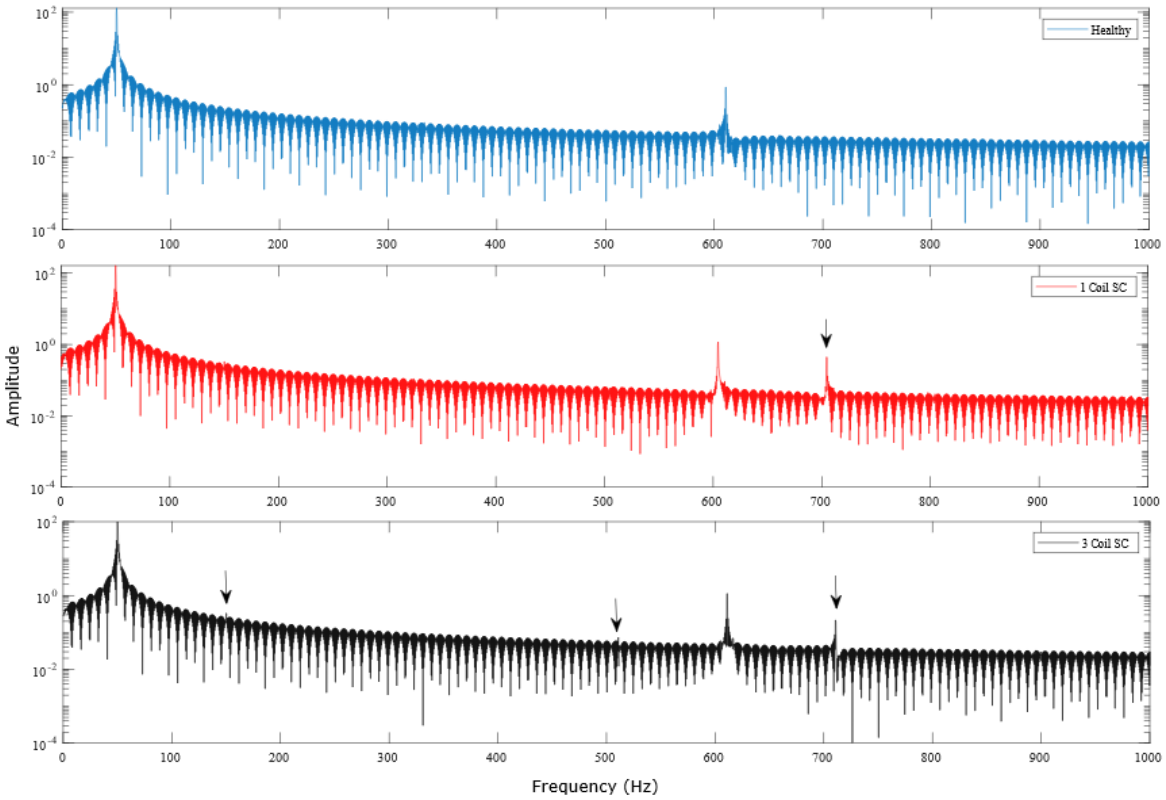

Figure 14 Space-vector of three-phase current (0 - 1000)

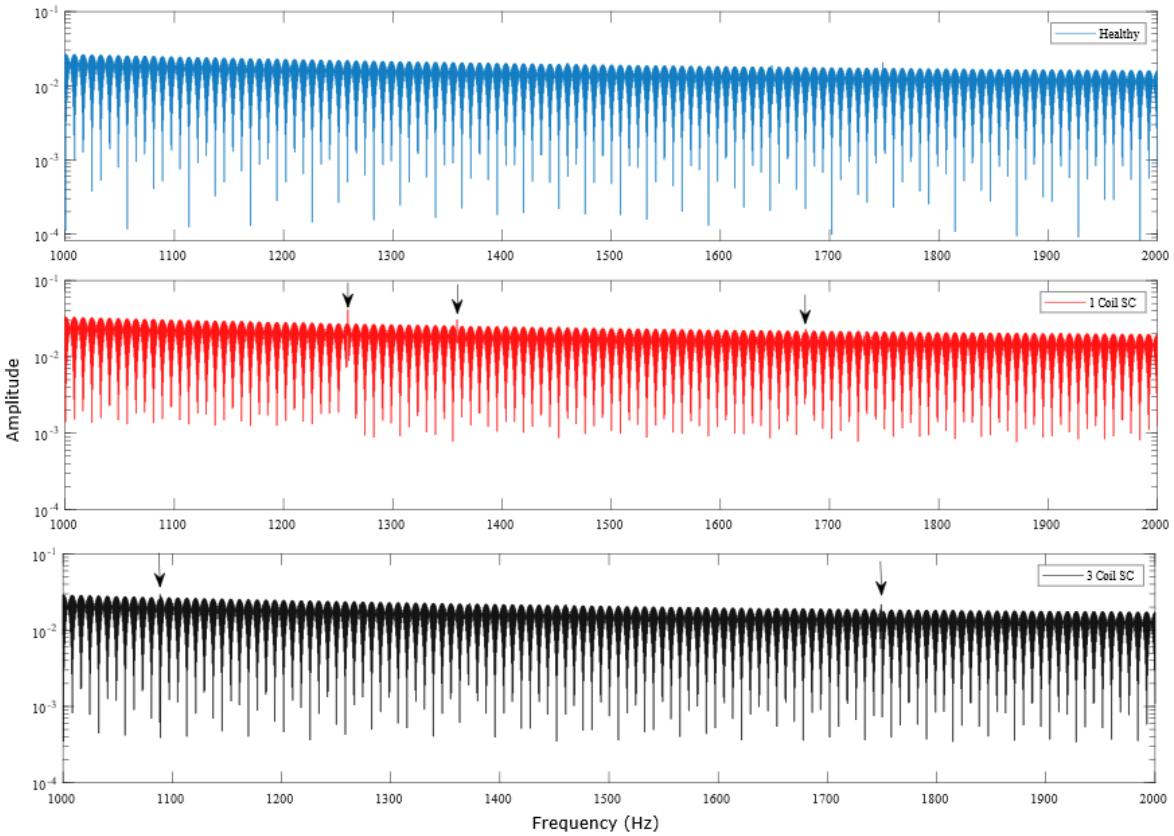

Figure 15 Space-vector of three-phase current (1000 - 2000)

Simulation with one coil of the stator winding in short circuit was also performed. The obtained spectrum is presented in figure 16. This figure clearly shows how harmonics appear due to this type of fault which are highlighted by black arrows. When some shorted turns are introduced, they are notorious for the appearance of the harmonics in the spectrum of the currents of the motor. The amplitude of these harmonics are higher than their surroundings, and their presence can be inferred from the FFT waveforms of the motor supply currents.

Another frequency spectrum of short-circuit between three coils is shown in figure 14 and 15. It indicates that the number of harmonics increases with the increase in turns of the coil (extension of fault). From the above figures, it is possible to observe the difference between healthy and faulty conditions of the IM. It is visible that the fault is detectable even when it is at an early stage of development. However, it should be noted that there are some differences between the spectra in figure 14 and 15, and conclusions can be done by comparing the higher number of harmonics as appeared in different results.

4.3.3 Park's Vector

The operating principle of the Park's vector (PV) is based on identifying unique signature patterns that are generated due to different conditions of the motor [26]. In this method, three motor currents are converted into two components called as (d−q) components by using PV transformation. The PV relies on the monitoring of the three-phase or line currents of the IM, namely i_a, i_b, and i_c.
The PV components, I_d and I_q, are calculated by [26]

$$i_d = \left(\frac{\sqrt{2}}{\sqrt{3}}\right) i_a - \left(\frac{1}{\sqrt{6}}\right) i_b - \left(\frac{1}{\sqrt{6}}\right) i_c \tag{4.1}$$

$$i_q = \left(\frac{1}{\sqrt{2}}\right) i_b - \left(\frac{1}{\sqrt{2}}\right) i_c \tag{4.2}$$

Under ideal conditions, i.e., for a healthy three-phase induction machine, the three-phase currents lead to a PV with the following components [26].

$$i_d = \left(\frac{\sqrt{6}}{\sqrt{2}}\right) \overline{1}_m \sin(\omega t) \tag{4.3}$$

$$i_q = \left(\frac{\sqrt{6}}{\sqrt{2}}\right) \overline{1}_m \sin\left(\omega t - \frac{\pi}{2}\right) \tag{4.4}$$

Where:

I_m - maximum value of the supply phase current (A)

ω - angular supply frequency (rad/s)

t - time variable (s)

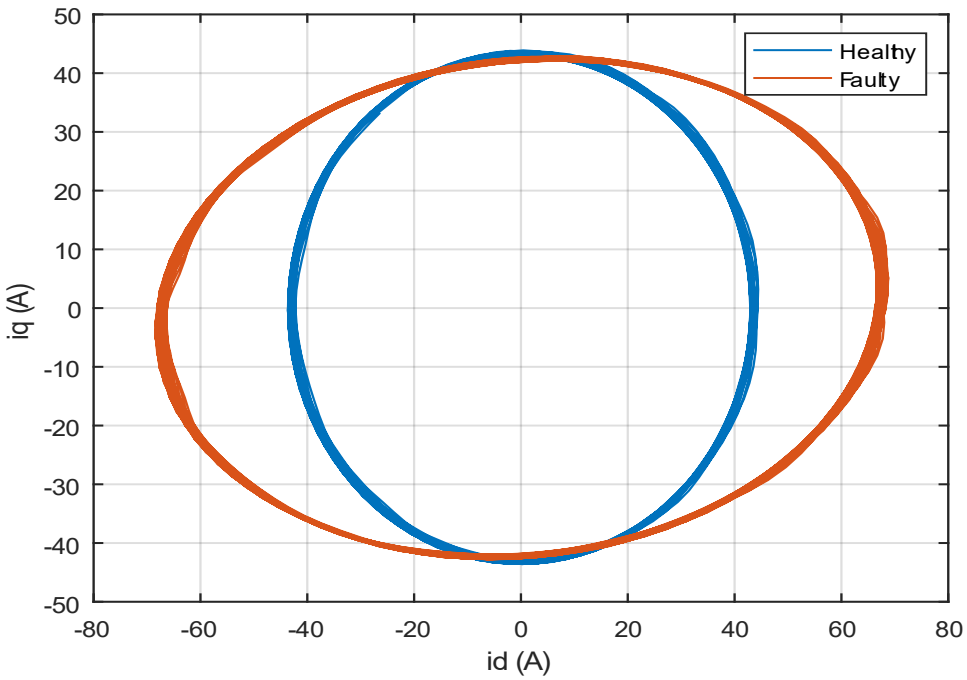

Figure 16 Park's Vector

The corresponding representation of the PV is the oval shape centered at the origin of the coordinates represented by blue color. In the case of stator inter-turn fault, the oval shape is distorted, which is indicated through orange color. The PV of different cases is shown in figure 16.

4.3.4 Torque and Speed

Introduction of faults directly affects the torque profile of the machine. Analyzation of the torque directly needs additional torque sensor. However, indirect analysis techniques such as, signal processing can be used to detect the faulty harmonics in the machine's torque profile. The electromagnetic torque in the air-gap is generated through the interaction between the rotor field and the stator winding field. The magnetic flux density in the air-gap is affected by the short circuit, and results in the development of more torque ripples and higher amplitude of slot harmonics [27]. The frequency-domain characteristic of torque is used to extract the distortion caused by a short circuit. In this technique, the torque time profile is transformed into the frequency to know the fault caused by a short circuit [27].

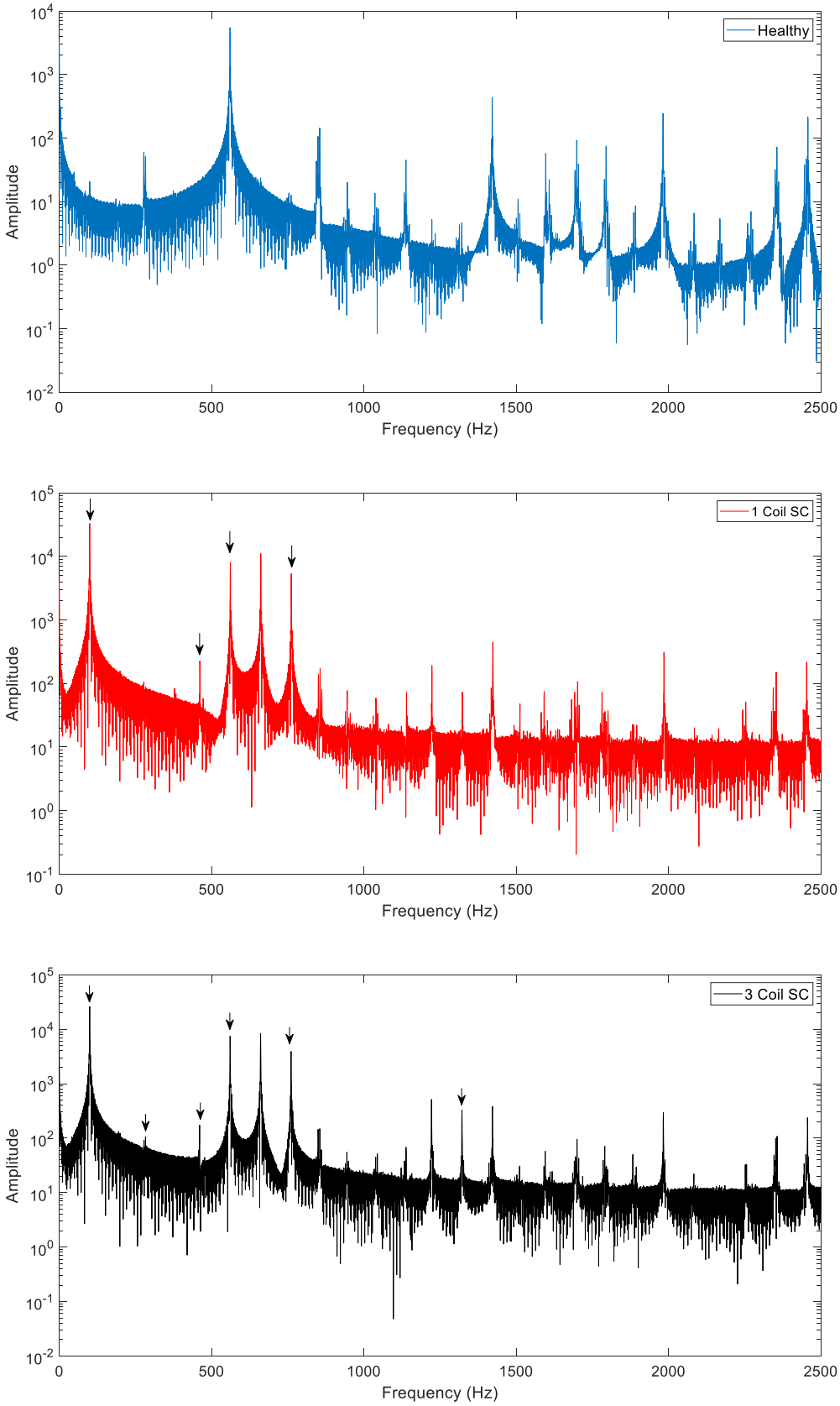

Figure 17 Frequency spectrum of Torque

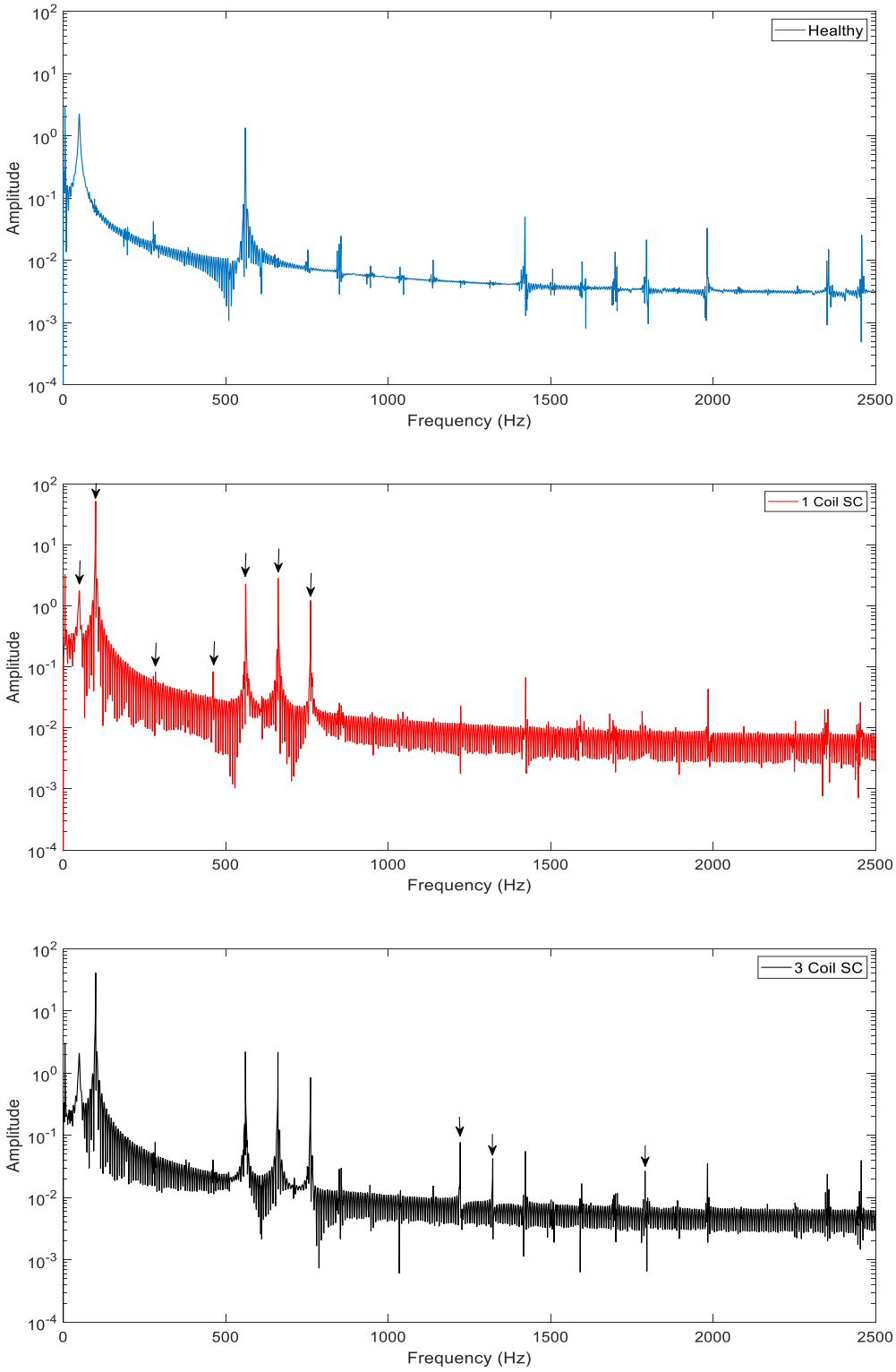

Figure 18 Frequency spectrum of Speed

The frequency spectrums of the torque in three various cases are shown in figure 17. From these graphs, one can easily distinguish the motor's healthy and faulty condition. As compare to torque amplitude in healthy, the harmonics and their amplitudes are higher during faulty cases which marked by black arrows. In addition, the analysis of

the electromagnetic torque developed by the motor in the presence of stator inter-turn short circuits reveals the presence of a significant harmonic. It should be emphasized that this electromagnetic torque is the one actually developed by the motor.

The frequency spectrum of the speed during three different conditions is shown in figure 18. During the healthy condition, IM runs smoothly, and there is no more oscillation in it. But when the short circuit fault occurs in the machine, the speed is going to affect. There is more oscillation which can see in figure 19. In this result, the time is taken during the steady-state condition of the motor. It is easy to understand the fault condition during the steady-state interval. The number of oscillations is increased with the extension of the fault area which marked by black arrows.

5 Conclusion

The author has carried out research to establish a reliable and easy diagnosis for SITF based on three-phase current space-vector, torque and speed results. The former method also has the advantage of being simple and having less data processing time. The expected result of this thesis was to give a reliable and straightforward diagnosis technique. For which initial IM had to be modelled and simulated.

Learning aspects of this thesis are enormous; the reason for that was the expected outcome. The solution is developed with various constraints, which include IM design, simulation and signal processing. In this thesis, the FEM based environment was used to solve the IM. The comparison of different results distinguishes the motor's healthy and faulty condition. To get these results, MATLAB program was used to perform space-vector and FFT.

The various results of three-phase current, torque and speed in faulty cases contain additional harmonics as compared to a healthy case. These all results indicate the inter-turn fault in the stator and differentiate the IM for a different state.

5.1 Future Work

The different tests and experiments have been left for the future work, because of lack of time. There are some improvements that could be done in order to achieve better results. The future work consists, actual stator rewinding of the IM, and author has to short the number of specific turns to get the results for faulty case. In addition, author can also try new diagnostic techniques for stator inter-turn fault.

6 Summary

6.1 English

Induction motors have an impact on almost every aspect of modern living. It is a sophisticated electro-mechanical device utilized in most industrial applications for the conversion of energy from electrical to mechanical form. Electric motors are the biggest consumer of electricity because of their consumption is around 60% of global power. Electrical motors are associated with various parts that are always prone to failures. The stator is one of the significant fault areas in an induction motor. Early monitoring and diagnosis of the faults have significant advantages like the safety of the operator, reducing production time loss, and minimizing the expensive maintenance and repair cost.

The work has been carried out with Finite element-based simulation. The studied model takes its geometrical and materials characteristics from a 400 V, 7.5 kW, 50 Hz, 3-phase induction motor. In order to create an induction motor according to the datasheet, used INFOLYTICA (MagNet) software. After completing the different steps such as wireframe model, assigning different materials for different parts, stator and rotor coils connection, the final healthy IM model is modelled. FEM mesh created by the analyst before finding a solution to a magnetic problem using FEM.

To verify the considered diagnostic methods, several healthy and fault conditions in the simulation were introduced. In this simulation, three types of analysis were used. Firstly, the healthy motor, secondly one coil short circuit, and lastly three coil short circuit. Simulation tests were performed using the MATLAB program for space-vector as well as for FFT method with 5 kHz sampling frequency to get the spectrum.

Different results of the flux distribution, three-phase current, torque and speed were compared for healthy as well as the faulty condition of induction motor. During the faulty case, there are more harmonics appear in the spectrum of the current and torque, and oscillation in the spectrum of the speed also increased. From these all, conclusions can be done by comparing the higher number of harmonics as appeared in different results. Two different shapes of the Park's vector also indicate the short circuit fault.

6.2 Estonian

Asünkroonmootorid mõjutavad peaaegu kõiki tänapäevaseid aspekte. See on keerukas elektromehaaniline seade, mida kasutatakse enamikes tööstuslikes rakendustes energia muundamiseks. Sellised elektrimootorid on maailma suurimad elektritarbija, kuna nende tarbimine moodustab umbes 60% kogu maailmas tarbitavast energiast. Asünkroonmasina üheks peamiseks osaks on staator. Rikete varaseks jälgimiseks ja diagnoosimiseks on palju eeliseid, mis tagavad operaatori ohutust, tootmise ajakulu vähendamist ning kallite hooldus- ja remondikulude minimeerimist.

Töö teostati lõpliku elemendil põhineva simulatsioonil. Uuritud kolmefaasilisel mootoril on järgmised parameetrid: 400 V, 7,5 kW, 50 Hz. Asünkroonmootori loomiseks kasutati tarkvara INFOLYTICA (MagNet). Pärast olid teostatud erinevad sammud, nagu traatkarkassi modelleerimine, erinevatele osadele materjalide määramine, staatori ja rootori mähiste ühendamine lõpliku mootori modelleerimine. Magnetprobleemile lahenduse leidmiseks oli kasutatud FEM tarkvara.

Kasutatud sellises uuringus diagnostiliste meetodite kontrollimiseks olid teostatud erinevad katsed. Antud uuringu raames olid tehtud kolm erinevat katset kolme erineva mootori seisundiga: terve mootor, mootor ühe lühiskeerguga, mootor kolme lühiskeerduga. Simulatsioonikatsed olid läbi viidud MATLAB tarkvara abil. Spektrite saamiseks oli teostatud kiire Fourier’ teisendus.

Uuringu raames olid võrreldud erinevad asünkroonmootori parameetrid: magnetvoo jaotus, kolmefaasiline vool, pöördemoment ja pöördekiirus. Vigase mootori korral ilmneb voolu ja pöördemomendi spektris rohkem harmoonilisi sagedusi ning samuti suureneb ka võnkumine kiiruse spektris. Tulemusi saab võrrelda suurendatud harmooniliste arvu abil. Lisaks sellele, Park’i vektori abil on võimalik tuvastada masinas oleva riket.

7 References

[1] B. Asad, T. Vaimann, A. Belahcen, A. Kallaste, "Broken Rotor Bar Fault Diagnostic of Inverter Fed Induction Motor Using FFT, Hilbert and Park's Vector Approach", XIII International conference of electrical machine, Greece, Sept. 2018.

[2] F. Duan, "Diagnostic of rotor and stator problems in industrial induction motor", school of electrical and electronic engineering, the university of Adelaide, Australia, August 2018.

[3] A. Sharma, S. Chatterji, L. Mathew and M. J. Khan, "Review of Fault Diagnostic and Monitoring Schemes of Induction Motors", International Journal for Research in Applied Science & Engineering Technology, vol.3, issue IV, April 2015

[4] B. K. Bose, "Modern power electronics and AC drives", Upper Saddle River, NJ: Prentice Hall, 2002.

[5] Induction motor fault diagnostic and monitoring methods - Scientific Figure on ResearchGate. Available from: https://www.researchgate.net/figure/A-two-pole-induction-motor-schematic_fig2_243055807 [accessed 15 May 2020].

[6] Induction Motor: Working Principle, Types, & Definition, [Online] Available: https://www.electrical4u.com/induction-motor-types-of-induction-motor/

[7] S. Barcellona, S. Negri and G. Superti-Furga, "Space-vector analysis of harmonic distortion in three-phase PWM," 2018 18th International Conference on Harmonics and Quality of Power (ICHQP), Ljubljana, 2018, pp. 1-6, doi: 10.1109/ICHQP.2018.8378943.

[8] Space Vector, [Online]. Available: http://people.ece.umn.edu/users/riaz/animations/spacevecmovie.html

[9] Z. Y. M. Hurtado, C. P. Tello and J. G. Sarduy, "A review on location, detection and fault diagnosis in induction machines", Journal of Engineering Science and Technology Review, vol.8, No.3, pp.185-195, 2015.

[10] Young-Jun Y, "Fault Detection of Induction Motor Using Fast Fourier Transform with Feature Selection via Principal Component Analysis," International Journal of Precision Engineering and Manufacturing, 2019.

[11] K. M. A. Alhassan, A. A. Obed and S. I. Hassan, "Stator Faults Diagnosis and Protection in 3-Phase Induction Motor Based on Wavelet Theory," Article in University of Baghdad Engineering Journal, vol.23, No.11, pp.138-157, November 2017.

[12]M. A. R. Alsaedi, "Fault diagnosis of three-phase induction motor: A review", Published only, Vol. 4, No. 1-1, 2015, pp. 1-8.

[13] L. Maraaba, Z. Al-Hamouz and M. Abido, "An Efficient Stator Inter-Turn Fault Diagnosis Tool for Induction Motors," article of energies 2018.

[14] E. Solodkiy, S. Salnikov and D. Dadenkov, "Detection Of Stator Inter-turn Short Circuit In Three-Phase Induction Motor Using Current Coordinate Transformation," IEEE 26th International Workshop on Electric Drives: Improvement in Efficiency of Electric Drives, Moscow, Russia. Jan 30 – Feb 02, 2019.

[15] S. E. Pandarakone, Y. Mizuno and H. Nakamura, "Online slight intern-turn short-circuit fault diagnosis using the distortion ratio of load current in a low voltage induction motor," IEEJ journal of industry applications, 29 March 2018, vol.7, no.6, pp.473-478.

[16] V. Hegde and M. G. Sathyanarayana Rao, "Detection of StatorWinding Inter-Turn Short Circuit Fault in Induction Motor Using Vibration Signals by MEMS Accelerometer", Article in Electric Power Components and Systems, vol.45, No.13, pp. 1463-1473, November 2017.

[17] W. Pietrowski and K. Górny, "Detection of inter-turn short-circuit at start-up of induction machine based on torque analysis", Research Article in open Physics, Vol. 15, Issue 1, pp. 851–856

[18] F. Zidani, M. E. H. Benbouzid, D. Diallo, and M. S. Nait-Said, "Induction motor stator faults diagnosis by a current Concordia pattern-based fuzzy decision system," IEEE Transactions on Energy Conversion, vol. 18, pp. 469-475, 2003.

[19] A. Siddique, G. S. Yadava, and B. Singh, "A review of stator fault monitoring techniques of induction motors," IEEE Transactions on Energy Conversion, vol. 20, pp. 106-114, 2005.

[20] B. Asad, L. Eensalu, T. Vaimann, A. Kallaste and A. Rassõlkin "The FEM Based Modeling and Corresponding Test Rig Preparation for Broken Rotor Bars Analysis", IEEE 60th International Scientific Conference on Power and Electrical Engineering of Riga Technical University, 2019.

[21] J.Tinsley Oden, Finite element method, [Online]. Available : http://www.scholarpedia.org/article/Finite_element_method.

[22] Magnet, 2D/3D Electromagnetic field simulation software [Online]. Available: https://www.mentor.com/products/mechanical/magnet/magnet/features.

[23] Carunaiselvane. C, S. Jeevananthan, "Generalized procedure for BLDC motor design and substantiation in MagNet 7.1.1 software", International conference on computing, electronics and electrical technologies, Kumaracoil, India, 2012.

[24] Signal Processing, [Online]. Available: https://www.sciencedirect.com/topics/physics-and-astronomy/signal-processing.

[25] A. Mohammed, J. I. Melecio and S. Djurović, "Stator Winding Fault Thermal Signature Monitoring and Analysis by In Situ FBG Sensors," in IEEE Transactions on Industrial Electronics, vol. 66, no. 10, pp. 8082-8092, Oct. 2019, doi: 10.1109/TIE.2018.2883260.

[26] K. N. Gyftakis and A. J. M. Cardoso, "A new space vector approach to detect stator faults in induction motors," *2017 IEEE Workshop on Electrical Machines Design, Control and Diagnosis (WEMDCD)*, Nottingham, 2017, pp. 232-237, doi: 10.1109/WEMDCD.2017.7947752

[27] Ullah, Z.; Hur, J. A Comprehensive Review of Winding Short Circuit Fault and Irreversible Demagnetization Fault Detection in PM Type Machines. *Energies* 2018, *11*, 3309.

Appendix 1

Datasheet of the Induction motor

3	Machine type (Squirrel cage induction machine)
4	Number of poles
3	Number of phases
1	Number of parallel paths (poles are connected in parallel)
144	Number of conductors in a stator slot
36	Number of turns
4	Number of conductors in turn
1	Number of layers of the stator winding
7/8/8/8/8/7/-II-	Coil pitch in slot pitches (←A/A→/A→; ←B'/←B'/B'→; ...)
50	Frequency of the supply voltage
0.155	Effective length of the machine
0.155	Length of the stator lamination
0.155	Length of the rotor lamination
0.300	Half of the average length of a coil with 7 pitches
0.312	Half of the average length of a coil with 8 pitches

Stator Parameters

220.0E-03	Outer diameter of the stator core
135.95E-03	Inner diameter of the stator core
36	Number of stator slots
4	Index for the shape of the stator slots
2.0E-03	H1 (Refer maps of stator slots)
0.85E-03	H11
14.30E-03	H13
3.0E-03	B11
5.85E-03	B12
8.50E-03	B13

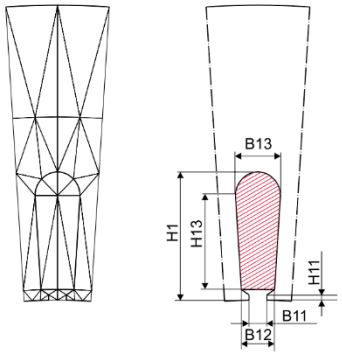

Rotor Parameters

135.0E-03	Outer diameter of the rotor core
45.0E-03	Inner diameter of the rotor core
28	Number of rotor slots
1	Index for the shape of the rotor slots
25.40E-03	H2 (Refer maps of rotor slots)
0.50E-03	H21
21.00E-03	H23
0.00E-03	B21
6.75E-03	B22
2.00E-03	B23

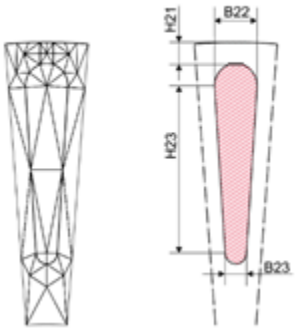

TABLE I

MAIN PARAMETERS OF THE MACHINE UNDER INVESTIGATIONS

Parameter	**Value**
Number of poles	4
Number of phases	3
Connection	Star/Delta
Number of stator slots	36; non-skewed
Number of rotor slots	28; skewed
Terminal voltage	690V/400V @50 Hz
Rated current	15.3A/8.8A
Rated power	7.5 kW@50 Hz

Appendix 2

Stator coils connection during healthy case.

Three Phases namely V2,V3 and V4.

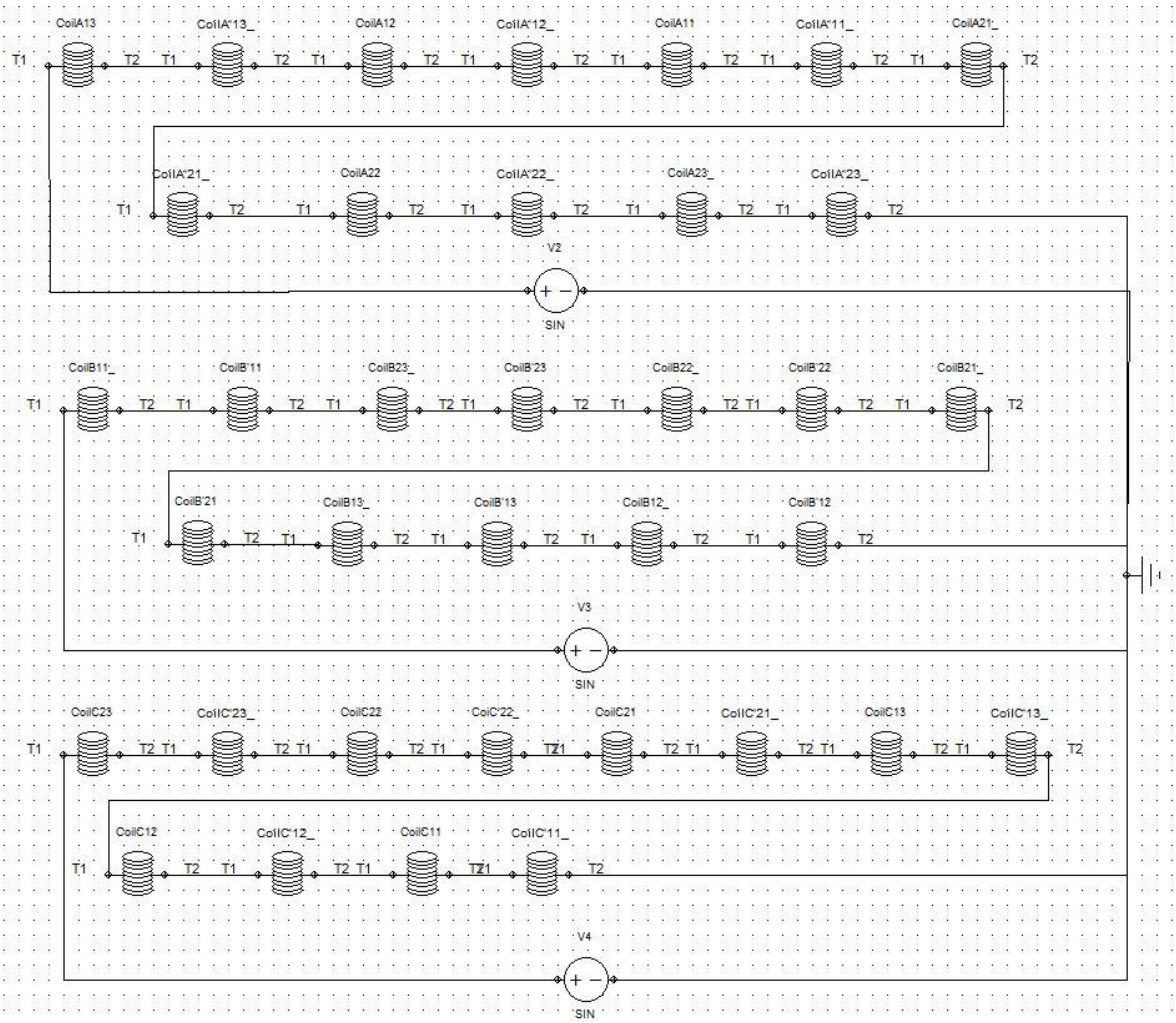

Appendix 3

Side view of the motor